International Journal of Control and Automation
Vol.9, No.3 (2016), pp.417-434
http://dx.doi.org/10.14257/ijca.2016.9.3.39

Adaptive Robust Backstepping (ARB) Control for Quadrotor Robot in Presence of Payload Variation and Unknown Disturbances

Wang Chen[1]*, Song Bifeng[1] and Meyer Nahon[2]

1 School of Aeronautics, Northwestern Polytechnical University, Xi'an 710072, China, 252430048@qq.com
2 Department of Mechanical Engineering, McGill University, Montreal, Canada.

Abstract

In this paper an adaptive robust control scheme along with its simulation on quadrotor is presented to deal with payload variation and unknown disturbance. Parametric and nonparametric uncertainties in the quadrotor model always make it difficult to design a controller to meet the performance requirement in various conditions during flight time. Adaptive robust backstepping (ARB) control, which is based on improved Lyapunov theory, is suggested to solve the problem. The proposed control scheme introduces piecewise functions into parameter adaptation law and control law to avoid control chattering while the Lyapunov function uniformly bounded is used. This choice not only provides guaranteed transient and asymptotic tracking performance but also precisely estimates the system parameters. Promising simulation results in different environments are carried out to demonstrate the efficiency and robustness of ARB control, and its advantages are indicated in comparison with conventional PID controller.

***Keywords**: Quadrotor robot, adaptive robust backstepping control, parameter estimation*

Introduction

In recent years, with their low cost and surveillance capabilities, small quadrotors have widespread applications in both military and civilian field. Current implementation includes terrain mapping, film shooting (with payloads like cameras and other special sensors), short distance delivery (with goods, military equipment or medicine), emergency damage assessment (nuclear facilities, earthquake, and floods) and etc. In missions above, quadrotors sometimes work in tough environment such as mountains, sea surface, or even deserts. Disturbance like sudden-come-in wind gust will bring degradation of performance or even crash. Some missions require quadrotors to be able to pick up/drop off payloads without significant degradation of performance. In this process, precise online parameter estimation (mass and moment of inertia) is also desirable, which is crucial information for manipulator to make decision. Good command tracking performance is another desirable property of quadrotor to keep away from obstacles like trees, buildings or mountains. Under this background, a robust and reliable control system should be developed to guarantee the tracking performance of vehicle in presence of payload variation and disturbance meanwhile provide precise estimation of system parameters.

Because of the involvement of nonlinearity and uncertainty, quadrotor is a complex underactuated system. Many prior works have proposed a varieties of control strategies for quadrotors. The PID control is widely implemented on quadrotors because of its simple structure, and it is also used as comparison for other control methods [1-4]. Backstepping control is also widely implemented on quadrotors to improve tracking performance [5-8], sometimes integral terms is integrated in backstepping to eliminate

ISSN: 2005-4297 IJCA

potential steady state error, which is shown to be valid in both simulation and experiments in.

Moreover, many researchers have focused on stabilization of quadrotors under disturbance such as wind gust. As in [10], sliding-mode adaptive controller is proposed to make quadrotor robust to 2D wind meanwhile estimate the disturbance. In [11], a PD and robust compensating combine [9]d controller is designed to deal with disturbance occur in taking-off and landing, tracking error is designed to be globally uniformly ultimately bounded. An integral predictive/nonlinear H_∞ controller is presented in [12], in which aerodynamics disturbance, parametric and structural uncertainties are considered, the controller is a hierarchical scheme, a model predictive controller (MPC) is designed for generating trajectory, a H_∞ controller is developed for stabilize the rotational movements.

As mentioned above, the capability of picking up/drop off payloads is crucial for accomplishment of certain mission such as short distance delivery or rescue. Therefore, precisely estimating the parameters of new system and keeping stability of quadrotor after payload is added on/dropped off is desirable. Many researchers have made effort on this field. Kermain proposes [13] a robust state estimator based on high order sliding mode to tackle the variation of mass and moment of inertia caused by payload variation. In [14], Fang and Gao present an new Lyapnov function including the error between real mass and estimated mass to deal with mass variation and constant disturbance, by choosing adequate control input and mass adaptation law, the asymptotical stability of system is guaranteed. In [15], Min designs an adaptive robust controller for altitude motion of quadrotor, a nonlinear robust structure is proposed at first to guarantee the stability and performance under certain boundness of mass and disturbance, and then adaptation law with projection is introduced to reduce the uncertainty and improve performance. In [16], Coza used fuzzy adaptive control to deal with model uncertainty and unknown payloads. In his work, alternate adaptive parameter method is implemented to instead of using e-modification to avoid chattering and parameter drifting.

1.1 Paper Contribution

Overall, the requirements of quadrotor control in various environments can be listed as:

(1) Precisely track the command with guaranteed performance

(2) Adapt to payload variation and keep stability of quadrotor

(3) Precisely estimate the system parameter

(4) Robust to unknown bounded disturbance

All the previous work mentioned has been proved to perform well under three requirements at most. The novelty of this work is satisfying the all the four requirements above at the same time, which is meaningful for future implementation. Another interesting part is the introduction of thrust model, which is helpful for investigating the behavior of propellers under various environments, which is seldom mentioned by other articles. The structure of this paper is organized as follows. In section 2, fundamental concept of quadrotor is introduced at first, and then the dynamics model under parameter variation and disturbance is formulated. In section 3, adaptive robust backstepping control is developed. A close loop Lyapunov function is proposed, by adequately choosing control law and parameter adaptation law, the tracking error is guaranteed to be globally uniformly ultimately bounded (GUUB), both transient and asymptotic performance of this control method is presented. In section 4, the simulation results are presented under various cases to verify the effectiveness and robustness of controller. Conclusion of this work is presented in section 5. The derivation process of attitude control is presented in appendix.

2. System Modeling

2.1 Quadrotor Description

Firstly, the orthogonal right-handed reference frames where the overall motion of flying robot evolves are defined as follows (figure 1):

-$[x_e, y_e, z_e]^T$ defines the earth-fixed frame.

-$[x_0, y_0, z_0]^T$ defines the quadrotor body-fixed frame.

-$[\phi, \theta, \psi]^T$ are three Euler angles (roll, pitch, and yaw) which define the attitude of quadrotor.

Quadrotor has 2 pairs of propellers, propellers 1 and 3 rotate in counter clockwise, and propellers 2 and 4 rotate clockwise. Unlike the conventional helicopter which can changes lift direction by controlling the pitch angle of the propeller, motion of quadrotor is controlled by varying the speed of four rotors. With 6 degrees of freedom but only 4 inputs, the quadrotor is an under-actuated system, the 4 system states components which can be controlled directly are attitude angles and altitude.

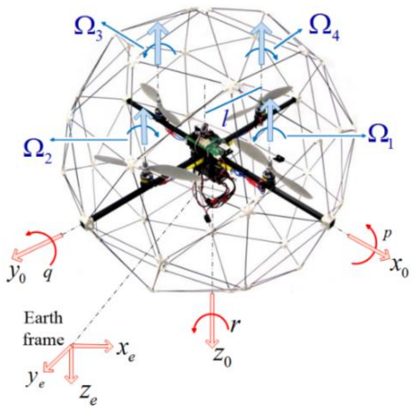

Figure 1. Definition of Frame

2.2 Dynamics Equation of Motion

1) Thrust model

The thrust and reaction torque generated by each propeller are proportional to rotation speed square of each motor Ω, which are expressed as :

$$T = k_t \Omega^2 \quad (1)$$

$$Q = k_q \Omega^2 \quad (2)$$

where T is thrust generated by propeller, k_t is the thrust coefficient, Q is the reaction torque, and k_q is the reaction torque coefficient.

2) Equation of Motion

Several assumptions are made in order to simplify the airframe model introduced as follows:

(1) The body of quadrotor system (even after payload added on) is rigid and symmetrical.

(2) The four propellers are rigid, no blade flapping occurs.

(3) Four propellers work under same environment at any time, which means k_t and k_q are always same for each propeller and keep to be constant.

(4) The quadrotor always work at small attitude angle.

These assumptions are reasonable because quadrotor always operates at low speed and small attitude angle. We define an earth frame and a body frame, and use Euler angle to express the attitude of the quadrotor. The dynamics model of quadrotor can be formulated as:

$$\begin{bmatrix} \dot{\phi} \\ \ddot{\phi} \\ \dot{\theta} \\ \ddot{\theta} \\ \dot{\psi} \\ \ddot{\psi} \\ \hline \dot{x} \\ \ddot{x} \\ \dot{y} \\ \ddot{y} \\ \dot{z} \\ \ddot{z} \end{bmatrix} = \begin{bmatrix} \dot{\phi} \\ \dot{\theta}\dot{\psi}\frac{I_{yy}-I_{zz}}{I_{xx}} + \dot{\theta}\frac{J_r}{I_{xx}}\Omega_r + \frac{1}{I_{xx}}u_2 \\ \dot{\theta} \\ \dot{\phi}\dot{\psi}\frac{I_{zz}-I_{xx}}{I_{yy}} + \dot{\phi}\frac{J_r}{I_{yy}}\Omega_r + \frac{1}{I_{yy}}u_3 \\ \dot{\psi} \\ \dot{\theta}\dot{\phi}\frac{I_{yy}-I_{xx}}{I_{zz}} + \frac{1}{I_{zz}}u_4 \\ \hline \dot{x} \\ \frac{(\cos\phi\sin\theta\cos\psi + \sin\phi\sin\psi)u_1}{m} \\ \dot{y} \\ \frac{(\cos\phi\sin\theta\sin\psi - \sin\phi\cos\psi)u_1}{m} \\ \dot{z} \\ g - \frac{\cos\phi\cos\theta}{m}u_1 \end{bmatrix} + \begin{bmatrix} 0 \\ \frac{1}{I_{xx}}d_\phi \\ 0 \\ \frac{1}{I_{yy}}d_\theta \\ 0 \\ \frac{1}{I_{zz}}d_\psi \\ \hline 0 \\ \frac{d_x}{m} \\ 0 \\ \frac{d_y}{m} \\ 0 \\ \frac{d_z}{m} \end{bmatrix} \tag{3}$$

In above equation, $[x,y,z]$ represents the position in earth frame, $[\phi,\theta,\psi]$ are attitude angles, $[I_{xx},I_{yy},I_{zz}]$ is airframe inertia matrix, J_p is moment of inertia of each propeller, d_z is bounded altitude disturbance, and d_ϕ , d_θ , d_ψ are bounded attitude disturbance of roll and pitch motion respectively. All of the disturbance are bounded and the boundaries are known explicitly, $|d_z| < D_z$, $|d_\phi| < D_\phi$, and $|d_\theta| < D_\theta$, $\Omega_r = \sum_{i=1}^{4}\Omega_i$, $|\phi| < \pi/2$, $|\theta| < \pi/2$, and $|\psi| < \pi/2$. During the fight, mass m and moments of inertia (I_{xx} , I_{yy} , and I_{zz}) of the quadrotor might change with picking up/dropping off the payload.

$[u_1,u_2,u_3,u_4]$ are force and moment input generated by propellers, and the relationship between $[u_1,u_2,u_3,u_4]$ and rotation speed of motors is $[\Omega_1,\Omega_2,\Omega_3,\Omega_4]$ as follows:

$$\begin{bmatrix} u_1 \\ u_2 \\ u_3 \\ u_4 \end{bmatrix} = \begin{bmatrix} k_t & k_t & k_t & k_t \\ lk_t & 0 & -lk_t & l \\ 0 & -lk_t & 0 & lk_t \\ -k_q & k_q & -k_q & k_q \end{bmatrix} \begin{bmatrix} \Omega_1^2 \\ \Omega_2^2 \\ \Omega_3^2 \\ \Omega_4^2 \end{bmatrix} \tag{4}$$

where l is the distance between center of gravity and each motor.

3. Control Strategy

3.1 System Structure

System is organized as shown in figure 2. Desired state block generates reference altitude and attitude for quadrotor. According to the feedbacks and references, controller calculates out adequate thrust and moment. Then this desired thrust and moment are allocated to motors by thrust allocation block, meanwhile the rotation speed of each motor is also calculated. Finally, motors generate thrust and moment to drive the aerial robot to desired states.

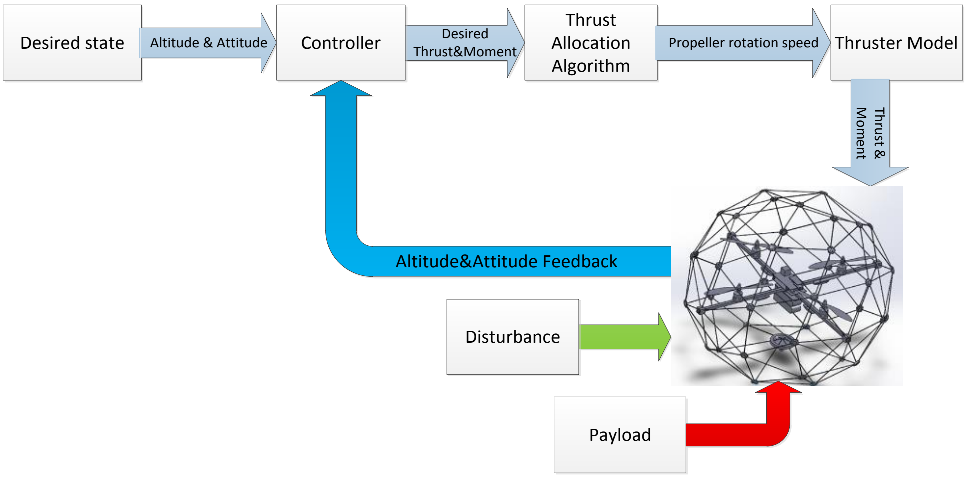

Figure 2. Structure of the System

3.2 Altitude Control

The challenges for controlling altitude motion are mass variation and force disturbance. The ideal control solution is to make the derivative of Lyapunov function strictly negative by choosing adequate control law and mass adaptation. z_r denotes the reference altitude.

Step I.

Define the error variable $e_1 = z_r - z$, then

$$\dot{e}_1 = z_r - z \tag{5}$$

Define $\dot{z} = v$ and $v = e_2 + \alpha_1$, α_1 is virtual velocity. e_2 represents error between real velocity v and virtual velocity α_1.

Then equation (5) is represented as:

$$\dot{e}_1 = \dot{z}_r - e_2 - \alpha_1 \tag{6}$$

Propose a candidate Lyapunov function V_1 for subsystem $e_1 = z_r - z$:

$$V_1 = \frac{1}{2} e_1^2 \tag{7}$$

The time derivative of equation (7) comes out to be:

$$\dot{V}_1 = e_1(\dot{z}_r - e_2 - \alpha_1) \tag{8}$$

Choose $\alpha_1 = \dot{z}_r + c_1 e_1$, where c_1 is positive design parameter. Then the derivative of

Lyapunov function becomes:

$$\dot{V}_1 = -c_1 e_1^2 - e_1 e_2 \tag{9}$$

From equation (9), the stability of altitude tracking error e_1 can be guaranteed if term $-e_1 e_2 = 0$.

Step II.

From equation (5) and altitude dynamics motion in equation (3), we can get:

$$\begin{aligned} \dot{e}_2 &= v - \dot{\alpha}_1 \\ &= g + \frac{1}{m}(U + d_z) - \ddot{z}_r - c_1 \dot{e}_1 \end{aligned} \tag{10}$$

Here let $U = u_1 \cos\theta \cos\phi$ for simplification, we propose an extended Lyapunov function as:

$$V_2 = V_1 + \frac{1}{2} e_2^2 + \frac{1}{2\gamma m}(m - \hat{m})^2 \tag{11}$$

Then derivative of equation (11) becomes:

$$\begin{aligned} \dot{V}_2 &= \dot{V}_1 + e_2 \cdot \dot{e}_2 - \frac{1}{\gamma m}(m - \hat{m})\dot{\hat{m}} \\ &= -c_1 e_1^2 - e_1 e_2 + e_2 (g + \frac{1}{m} U + \frac{d_z}{m} - \ddot{z}_r - c_1 \dot{e}_1) - \frac{1}{\gamma m}(m - \hat{m})(\dot{\hat{m}}) \end{aligned} \tag{12}$$

Define $T = -e_1 e_2 + e_2 (g - \ddot{x}_r - c_1 \dot{e}_1)$ and let $\dot{\hat{m}} = \gamma T$. γ denotes adjustable parameter which is used for changing the parameter adaptation speed. Then let $m - \hat{m} = \tilde{m}$, equation (12) will be rewritten as

$$\begin{aligned} \dot{V}_2 &= -c_1 e_1^2 + B + \frac{e_2}{m}(U + d_z) - \frac{1}{m}\tilde{m}T \\ &= -c_1 e_1^2 + \frac{\hat{m}}{m}T + \frac{e_2}{m}(U + d_z) \end{aligned} \tag{13}$$

Choose $U = -c_2 e_2 - \hat{m}T/e_2 - D_z \cdot sign(e_2)$, where c_2 is a positive design parameter. D_z is the boundary of disturbance, which means $|d_z| < D_z$. $\dot{V}_2$ will become:

$$\begin{aligned} \dot{V}_2 &= -c_1 e_1^2 - c_2 e_2^2 + \frac{1}{m}\left[d \cdot e_2 - D \cdot sign(e_2) \cdot e_2\right] \\ &= -c_1 e_1^2 - c_2 e_2^2 + \frac{1}{m}\left(d \cdot e_2 - D|e_2|\right) \end{aligned} \tag{14}$$

Because $d \cdot e_2 - D|e_2| < 0$, then

$$\dot{V}_2 < 0 \tag{15}$$

In the derivation process above, with the introduction of $sign(e_2)$, $\dot{V}_2$ becomes strictly negative as shown in equation (15). As a result, the system seems to be able to asymptotically track the reference by using the control law and mass adaptation law presented above. However, the $sign(e_2)$ is impossible be precisely acquired, because condition $e_2 = 0$ can never be reached, which will cause the $sign(e_2)$ jump between -1 and 1 all the time. Therefore, chattering of control input u_1 will occur, which will finally result in the chattering of propeller rotation speed, and all of these are undesirable in both simulation and experiments. As shown in figure 3, propeller rotation speed from $t = 2s$ to

$t = 2.5s$ is shown as an example. In this process, although quadrotor is able to precisely track the reference, the rotation speed of propellers jumps periodically between around $520 rad/s$ and $560 rad/s$.

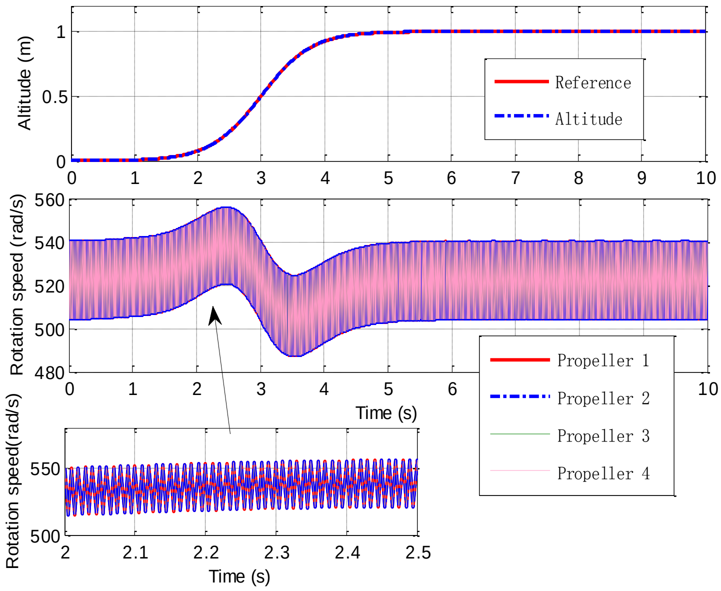

Figure 3. Chattering of the Propeller Rotation Speed

In order to overcome this chattering problem, modifications are made based on previous control strategy, which use piecewise continuous function to replace $sign(e_2)$. Instead of making Lyapunov function strictly negative, the core principle of the new strategy is making the Lyapunov function uniformly bounded. This method can be achieved by introducing two following piecewise functions into control law and mass adaptation law developed above.

First piecewise function $f(\cdot)$ is formulated as:

$$f(x) = \begin{cases} 0, & x < 1 \\ x - 1, & 1 < x < 2 \\ 1, & x > 2 \end{cases} \tag{16}$$

This function has the property as:

$$f\left(\frac{|\hat{m}|}{m_{\max}}\right)\hat{m}\tilde{m} \le -\frac{\tilde{m}^2}{2} + \frac{m^2}{2} < -\frac{\tilde{m}^2}{2} + \frac{m_{\max}^2}{2} \tag{17}$$

The reason for introducing $f(\cdot)$ is to introduce term $-\tilde{m}^2/2$ and another explicit number $m_{\max}^2/2$ into $\dot{V}_2$ inequality [17], which is helpful for building up relationship $\dot{V}_2 < -AV_2 + B$, where A and B are explicitly known numbers. In this way, V_2 will be guaranteed to be uniformly bounded, details of this derivation process will be shown in following paragraph.

Another piecewise function $sg(\cdot)$ is defined as equation (17), where ε is a positive design parameter.

$$sg(e_2)=\begin{cases}-1, & e_2<-\varepsilon \\ \dfrac{1}{\varepsilon}, & -\varepsilon\le e_2\le\varepsilon \\ 1, & e_2>\varepsilon\end{cases} \tag{18}$$

$sg(e_2)$ is a continuous function with adjustable parameter ε, which is used for changing the thickness of boundary layer around $e_2=0$. Then control law U and mass adaptation law $\dot{\hat{m}}$ can be choosen as:

$$U=-c_2e_2-\frac{T\hat{m}}{e_2}-D_z\cdot sg(e_2) \tag{19}$$

$$\dot{\hat{m}}=\gamma T-\sigma_m f(\frac{|\hat{m}|}{m_{\max}})\hat{m} \tag{20}$$

Finally, $\dot{V}_2$ can be acquired

$$\dot{V}_2=-c_1e_1^2-\frac{c_2}{m}e_2^2+\frac{e_2}{m}[d-D_z\cdot sg(e_2)]-\frac{\sigma_m}{\gamma m}\tilde{m}\hat{m}f(\frac{|\hat{m}|}{m_{\max}}) \tag{21}$$

The boundary of term $e_2\left[d-D\cdot sg(e_2)\right]$ in equation (21) is presented as

$$\begin{cases} e_2[d-D\cdot sg(e_2)]<0, & |e_2|>\varepsilon \\ e_2[d-D\cdot sg(e_2)]\le\dfrac{D_z\varepsilon+D_z}{m_{\min}}, & |e_2|\le\varepsilon \end{cases} \tag{22}$$

So overall, we get $e_2[d-D_z\cdot sg(e_2)]\le\frac{D_z\varepsilon+D_z}{m_{\min}}$. As a result, inequality of $\dot{V}_2$ is obtained as:

$$\dot{V}_2<-c_1e_1^2-\frac{c_2}{m}e_2^2-\frac{\sigma_m}{2m}\tilde{m}^2+\frac{D_z\varepsilon+D_z}{m_{\min}^2}+\frac{\sigma_m m_{\max}}{2} \tag{23}$$

So overall, we get $e_2[d-D_z\cdot sg(e_2)]\le\frac{D_z\varepsilon+D_z}{m_{\min}}$. As a result, inequality of $\dot{V}_2$ is obtained as:

$$\dot{V}_2<-AV_2+B \tag{24}$$

Integrate both side of inequality (24), and use the relationship $e^{-At}<1$ and $1-e^{-At}<1$. $V(t)$ is bounded by:

$$V_2(t)\le V_2(0)e^{-At}+\frac{B}{A}(1-e^{-At})\le V_2(0)+\frac{B}{A} \tag{25}$$

The inequality shows that $V(t)$ is globally ultimately uniformly bounded. This implies that e_1, e_2 and $\tilde{m}$ are bounded. Thus, the altitude and altitude velocity z, v and estimated mass $\hat{m}$ are also bounded, because $U=u_1\cos\theta\cos\phi$, control law of altitude motion u_1 can be obtained:

$$
\begin{aligned}
u_1 &= \frac{1}{\cos\theta\cos\phi}U \\
&= \frac{1}{\cos\theta\cos\phi}\left\{-c_2e_2 - \frac{[-e_1e_2 + e_2(g - \ddot{x}_r - c_1\dot{e}_1)]\hat{m}}{e_2} - D_a \cdot sg(e_2)\right\}
\end{aligned}
\tag{26}
$$

3.3 Performance Analysis

The transient and asymptotic altitude tracking error performance of e_1 can be acquired. the boundary of e_1 can be guaranteed. From equation (22) and (23), because $(c_2/m)e_2^2 \geq 0$ and $(\sigma_m/2m)\tilde{m}^2 \geq 0$, inequality of e_1 is obtained:

$$c_1e_1^2 < -\dot{V}_2 + B \tag{27}$$

Propose a transient performance standard $\frac{1}{T}\int_0^T e_1^2$, and combine equation (27), we obtain:

$$\frac{1}{T}\int_0^T e_1^2 < \frac{1}{c_1}\left(\frac{1}{T}\int_0^T -\dot{V}_2dt + B\right) \tag{28}$$

Because $\int_0^T -\dot{V}_2dt = V_2(0) - V_2(T)$, inequality (28) becomes

$$
\begin{aligned}
\frac{1}{T}\int_0^T e_1^2 &< \frac{1}{c_1}\left(\frac{V_2(0)-V_2(T)}{T} + B\right) \\
&< \frac{1}{c_1}\left(\frac{V_2(0)}{T} + B\right)
\end{aligned}
\tag{29}
$$

From inequality (29), transient performance $\frac{1}{T}\int_0^T e_1^2$ is defined by quadrotor robot initial state $V_2(0)$, B and design parameter c_1. With the time goes on, guaranteed performance will become better because term $V_2(0)/T$ decreases with time.

Asymptotic error performance can be acquired by letting $T \to \infty$ in equation (29). From equation (25), the tracking error is bounded, which means $\lim_{T\to\infty}\{V_2(0) - V_2(T)/T\} = 0$, as a result, asymptotic tracking performance can be presented as:

$$\lim_{T\to\infty}\frac{1}{T}\int_0^T e_1^2 < \lim_{T\to\infty}\frac{1}{c_1}\left(\frac{V_2(0)-V_2(T)}{T} + B\right) = \frac{B}{c_1} \tag{30}$$

From inequality (28), the transient tracking performance of ARB control can be characterized by function of initial state, design parameter c_1, γ, ε_1, σ_m and the disturbance boundary D_z. Larger c_1, γ and smaller ε_1, σ_m are helpful for improvement of transient tracking performance. Accurate priory estimation of disturbance boundary D_z will also decrease the transient error. From equation (29) and (30), 2 conclusions can be acquired as:

1. The asymptotic error performance is not related to initial state and mainly determined by the disturbance. Asymptotic error can be decreased by increasing c_1.
2. Over estimation of mass, which means term $|\hat{m}|/m_{\max} > 1$, term $\sigma_m m^2{}_{\max}/2$ will show up in B. This will degrade performance of both transient and asymptotic tracking.

3.4 Control of Attitude

The challenges of controlling the attitude angles are the variation of moment of inertia $[I_{xx}, I_{yy}, I_{zz}]$ caused by changes of payload, and the bounded moment disturbance $[d_\phi, d_\theta, d_\psi]$. Because the equations of motion of attitude and altitude are similar, same control strategy developed in altitude control can be applied. The small difference in control between altitude motion is additional function $sg(\cdot)$ is introduced in attitude control to deal with body gyros term such as $\dot{\theta}\dot{\psi}(I_{yy}-I_{zz})/I_{xx}$, in which $(I_{yy}-I_{zz})/I_{xx}$ is unknown and changed with payload. The control law and adaptation law can be formulated as:

$$\begin{cases} u_2 = -c_{2,\phi}e_{2,\phi} - \dfrac{(T_\phi - e_{2,\phi}\ddot{\phi}_r)\hat{I}_{xx}}{e_{2,\phi}} - D_\phi \cdot sg_{1,\phi}(e_{2,\phi}) \\ \quad -(\Delta I_\phi)_{\max} \cdot sg_{2,\phi}(\dot{\theta}\dot{\psi}e_{2,\phi}) - \dot{\theta}J_r\Omega_r \\ \dot{\hat{I}}_{xx} = \gamma_\phi T_\phi - \sigma_\phi f(\dfrac{|\hat{I}_{xx}|}{I_{xx,\max}})\hat{I}_{xx} \\ u_3 = -c_{2,\theta}e_{2,\theta} - \dfrac{(T_\theta - e_{2,\theta}\ddot{\theta}_r)\hat{I}_{yy}}{e_{2,\theta}} - D_\theta \cdot sg_{1,\theta}(e_{2,\theta}) \\ \quad -(\Delta I_\theta)_{\max} \cdot sg_{2,\theta}(\dot{\phi}\dot{\psi}e_{2,\theta}) - \dot{\phi}J_r\Omega_r \\ \dot{\hat{I}}_{yy} = \gamma_\theta T_\theta - \sigma_\theta f(\dfrac{|\hat{I}_{yy}|}{I_{yy,\max}})\hat{I}_{yy} \\ u_4 = -c_{2,\psi}e_{2,\psi} - \dfrac{(T_\psi - e_{2,\psi}\ddot{\psi}_r)\hat{m}}{z_{2,\psi}} - D_\psi \cdot sg_{1,\psi}(e_{2,\psi}) \\ \quad -(\Delta I_\psi)_{\max} \cdot sg_{2,\psi}(\dot{\phi}\dot{\theta}e_{2,\psi}) \\ \dot{\hat{I}}_{zz} = \gamma_\psi T_\psi - \sigma_\psi f(\dfrac{|\hat{I}_{zz}|}{I_{zz,\max}})\hat{I}_{zz} \end{cases} \quad (31)$$

where $T_i = -e_{1,i}e_{2,i} - e_{2,i}c_{1,i}\dot{e}_{1,i}$, $i = \phi,\theta,\psi$; $c_{1,i}$, $c_{2,i}$, σ_i , λ_i , $i = \phi,\theta,\psi$ are adjustable parameters, and they have similar definition as those in altitude control. $\left(\Delta I_\phi\right)_{\max} = \max\left(\left|I_{yy}-I_{zz}\right|\right)$, $\left(\Delta I_\theta\right)_{\max} = \max\left(\left|I_{zz}-I_{xx}\right|\right)$, $\left(\Delta I_\psi\right)_{\max} = \max\left(\left|I_{xx}-I_{yy}\right|\right)$. The attitude control laws and parameters adaptation laws are able to guarantee the attitude motion globally ultimately uniformly bounded.

3.5 Thrust Allocation Algorithm

The thrust allocation algorithm is introduced to investigate the behavior of propellers in presence of payload variation and disturbance. The thrust allocation algorithm distributes the desired vertical force and moments among the four thrusters:

$$\begin{cases} T_1 = -\dfrac{u_1}{4} + \dfrac{u_3}{2l} + \dfrac{u_4 k_t}{4k_q} \\ T_2 = -\dfrac{u_1}{4} - \dfrac{u_2}{2l} - \dfrac{u_4 k_t}{4k_q} \\ T_3 = -\dfrac{u_1}{4} - \dfrac{u_2}{2l} - \dfrac{u_4 k_t}{4k_q} \\ T_4 = -\dfrac{u_1}{4} + \dfrac{u_2}{2l} - \dfrac{u_4 k_t}{4k_q} \end{cases} \quad (32)$$

where T_i is the thrust of *ith* propeller.

Based on the thrust produced by the thrust allocation algorithm, we calculate a corresponding propeller RPM using:

$$\Omega_i = \sqrt{\frac{T_i}{k_t}} \tag{33}$$

Based on equation (33), desired rotation speeds of propellers are sent to motor to generate corresponding thrust and moment.

4. Simulation Results

Simulations are carried out to verify the control strategy. Mass of quadrotor is $m_{initial} = 1.5kg$, and initial inertia moment are $I_{xx} = I_{yy} = 0.03kg \cdot m^2$, $I_{zz} = 0.04kg \cdot m^2$. Mass of payload is $m_{payload} = 0.5kg$, moments of inertia after payload is added on are $I_{xx\_\text{added}} = I_{yy\_\text{added}} = 0.05kg \cdot m^2$, $I_{zz\_added} = 0.045kg \cdot m^2$. The inertia margins defined in section 3.4 are $\left(\Delta I_\phi\right)_{\max} = 0.01kg \cdot m^2$, $\left(\Delta I_\theta\right)_{\max} = 0.01kg \cdot m^2$, and $\left(\Delta I_\psi\right)_{\max} = 0.005kg \cdot m^2$. The thrust coefficient is acquired from experiments in [18], and $k_t = 1.34 \times 10^{-5} N \cdot rad^{-2} \cdot s^2$, $k_q = 3.136 \times 10^{-7} N \cdot m \cdot rad^{-2} \cdot s^2$.

The adjustable parameters are chosen as table below.

Table 1. Parameters in Simulation

i	$c_{1,i}$	$c_{2,i}$	λ_i	σ_i	$\varepsilon_{1,i}$	$\varepsilon_{2,i}$	D_i
Height z	1	0.2	0.4	1	0.025	None	3
Roll ϕ	0.1	0.3	10	1	0.01	0.005	0.02
Pitch θ	0.1	0.3	10	1	0.01	0.005	0.02
Yaw ψ	0.1	0.1	5	1	0.006	0.002	0.006

The desired state is a typical maneuver of quadrotor. Initial state of quadrotor is $[x, y, z] = [0,0,0]'$, and $[\phi, \theta, \psi] = [0,0,0]'$.which means quadrotor is stay at ground initially. Then this robot is commanded to track an altitude trajectory and rise to 1 meter high and then keep hovering. After around 1 second, quadrotor is commanded to track the desired attitude. The simulation results of this typical maneuver are presented in 4 different cases repectively.

(1) Absence of payload variation and disturbance
(2) Payload variation only
(3) Disturbance only
(4) In presence of payload variation and disturbance.

In each case, two figures are shown. The top figures in each case have 5 scopes. The top 4 scopes represent altitude and attitude angles during the maneuver. In each scope, simulation results controlled by ARB and PID are shown for comparison. The fifth scope shows the variation of propeller rotation speed calculated by ARB control.

In the second figure of each case, there are 4 scopes, which denote the variations of estimated mass and estimated moments of inertia generated by ARB control respectively.

4.1 Absence of Payload Variation and Disturbance

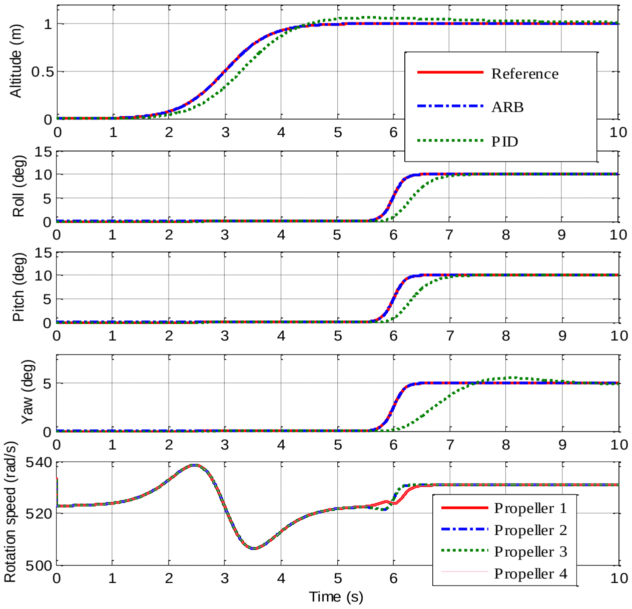

Figure 4. Tracking Performance and Propeller Rotation Speed in Case 1

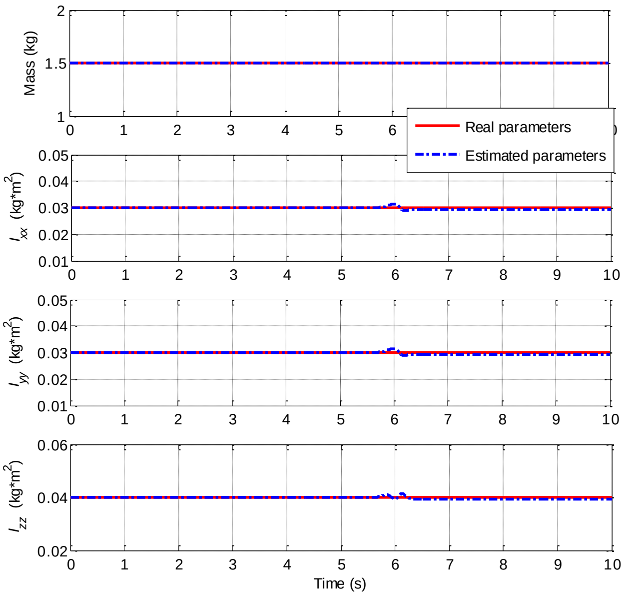

Figure 5. Estimation of Parameters by ARB Control in Case 1

From figure 4 and 5, compared with PID control, ARB control is able to precisely track the reference meanwhile estimate the parameter of system. The small differences between rotation speeds of propellers around $t = 6s$ are for tracking attitude angle.

4.2 Payload Variation Only

Payload $m_{payload} = 0.5kg$ is added on at $t = 6s$, the mass and moment of inertia of system changes immediately.

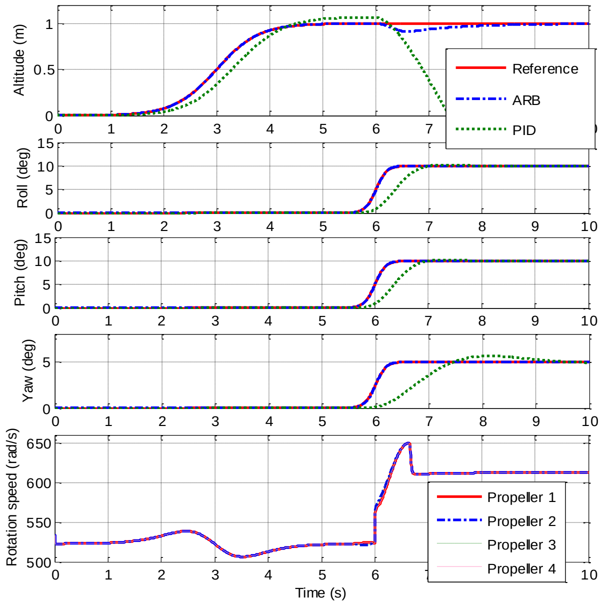

Figure 6. Tracking Performance and Propeller Rotation Speed in Case 2

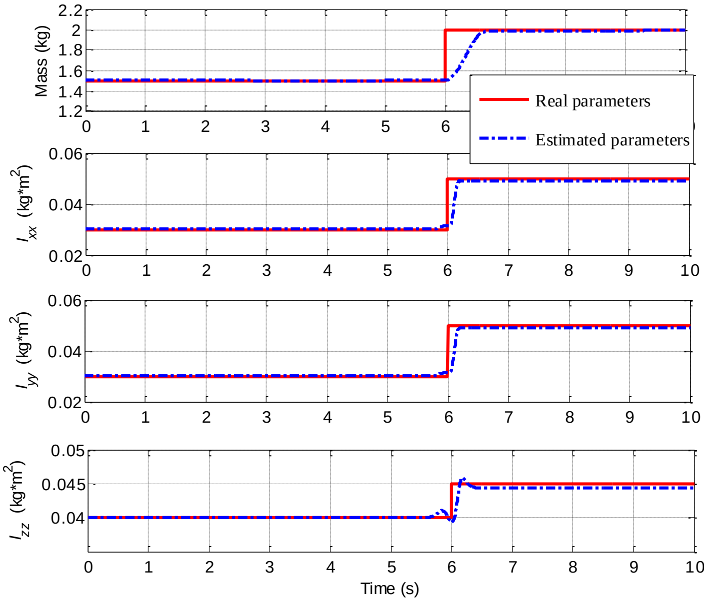

Figure 7. Estimation of Parameters by ARB Control in Case 2

In figure 6 and figure 7, after 0.5kg payload is added on, quadrotor controlled by PID descends rapidly and falls to ground within 2 seconds, which means the PID control is not able to generate enough thrust to resist new gravity, the performance of attitude tracking also degrade a little bit.

In terms of performance of ARB control, the rotation speed of propellers drastically increase after $t = 6s$ to generate adequate thrust, which denote that the controller manage to adapt to new gravity, and the altitude decreases by only 9 centimeters and recovers to 1 meter again within 2 seconds, meanwhile the estimate of mass reaches the real mass within 0.6 second. The ARB control also provide excellent attitude tracking performance and precise estimation of moment of inertia as shown in figure 7.

4.3 Disturbance Only

Bounded disturbance in each motion are described by sinusoidal functions. $d_z = 2.5\sin(2\pi t)$, $d_\phi = 0.015\sin(6\pi t)$, $d_\theta = 0.015\sin(6\pi t)$. $d_\psi = 0.006\sin(6\pi t)$. The disturbance is added on from $t = 0s$.

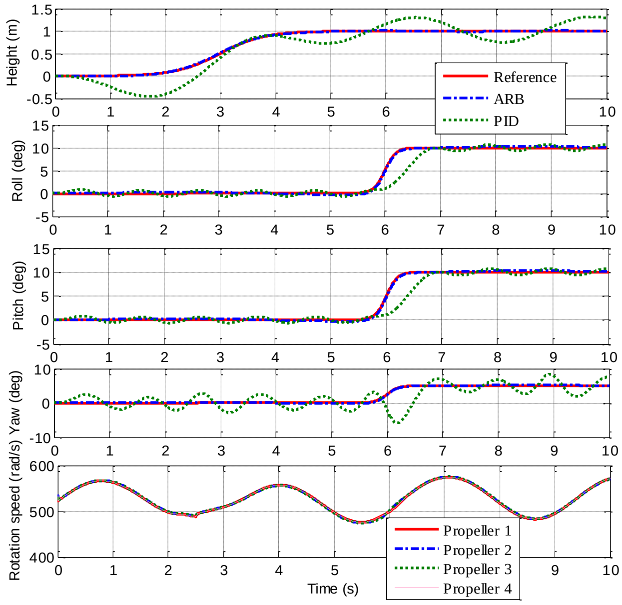

Figure 8. Tracking Performance and Propeller Rotation Speed in Case 3

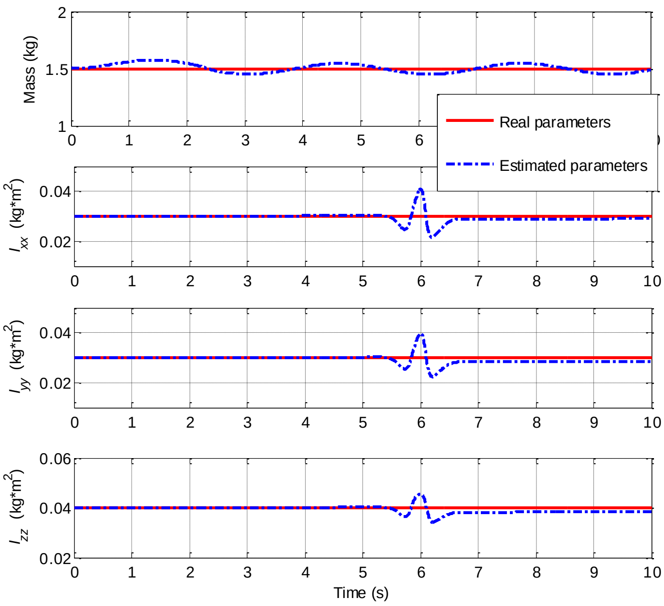

Figure 9. Estimation of Parameters by ARB Control in Case 3

In figure 8, under impact of disturbance, altitude of PID control fluctuate with amplitude up to 0.5 m, the yaw angle also shows sinusoidal like movement, which bring the degradation of performance.

In terms of ARB control, in figure 8, the rotation speed of propellers changes with the similar period as sinusoidal function of altitude disturbance $d_z = 2.5\sin(2\pi t)$, which means the ARB control is robust to disturbance by commanding propeller to generate sinusoidal like thrust and moment correspondingly to track reference under disturbance. In figure 8, under bounded disturbance, after experiencing larger estimation errors during attitude maneuver around $t = 6s$, ARB is able to estimate the mass precisely within maximum error of 90g, the estimated moment of inertia converge to real number after a small fluctuation during attitude maneuver.

4.4 Disturbance & Payload Variation

The combination impact of disturbance and payload variation is investigated in figure 10 and 11. Payload variation and disturbance is the same as in 2nd and 3rd case.

In figure 10, altitude of PID control fluctuates with disturbance at the beginning. After the payload is added on at $t = 6s$, quadrotor robot falls to ground similarly with situation in the 2nd case. Attitude controlled by PID is also similar to the 2nd case.

The ARB controller is adaptive and robust to payload variation and disturbance, as shown in figure 10, rotation speed of propeller is sinusoidal like from the beginning to resist disturbance, the slightly difference between propellers around $t = 6s$ is caused by attitude maneuver. After $t = 6s$, rotation speed of propeller increase drastically to adapt to new gravity, altitude decrease by 15 centimeters and recovers to 1m within 2.5 seconds. Finally, rotation speed of propeller is still sinusoidal like at around $600 rad / s$ than, which provides adequate thrust to support larger gravity and resist disturbance simultaneously. All of the parameters are precisely estimated within 1 second as shown in figure 11.

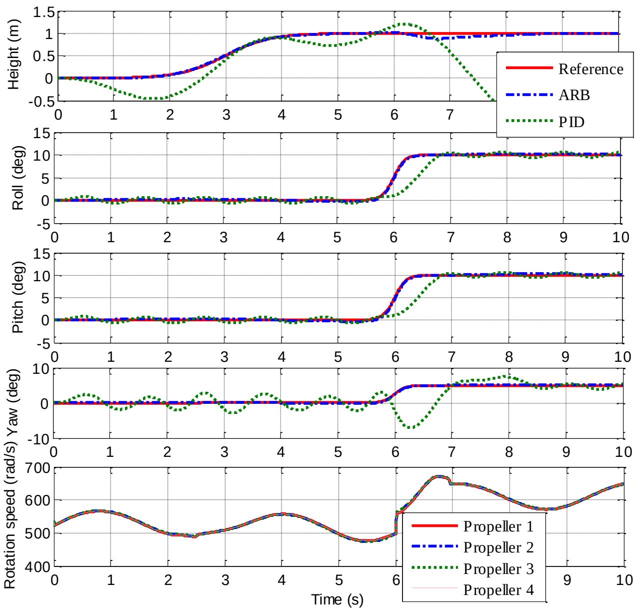

Figure 10. Tracking Performance and Propeller Rotation Speed in Case 4

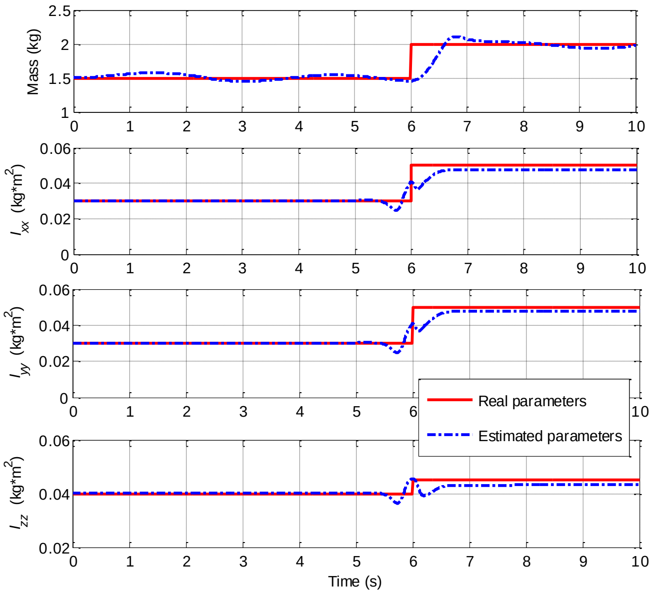

Figure 11. Estimation of Parameters by ARB Control in Case 4

5. Conclusion

An adaptive robust backstepping (ARB) controller is developed for quadrotor robot to control the altitude and attitude in presence of payload variation and unknown disturbances. In the designing process, both parametric and non-parametric uncertainties of model is considered, close loop Lyapunov function of system is then built up and guaranteed to be GUUB by choosing adequate control law and adaptation law. Simulation results are carried out to validate the control strategy, the results indicate that the control scheme provide excellent reference tracking performance in various conditions.

The control design presented in this paper is based on a quad-rotor robot, however, such scheme also can be applied to different miniature multi-rotor MAVs (eight-rotors and hexa-rotors), since they share similar kinematic and dynamic models.

References

[1] S. Bouabdallah, A. Noth and R. Siegwart, “PID vs LQ control techniques applied to an indoor micro quadrotor”, IEEE/RSJ International Conference on Intelligent Robotic and Systems, Jaan, vol. 3, September 28-October 2 **(2004),** pp. 2451-2456.

[2] J. Li and Y. Li, “Dynamic analysis and PID control for a quadrotor”, International Conference on Mechatronics and Automation, China, August 7-10 **(2011)**, pp 573-578.

[3] L.A. Salih, M. Moghavvemi, H.A.F. Mohamed and K.S. Gaeid, “Modelling and PID controller design for a quadrotor unmanned air vehicle”, IEEE International Conference on Automation Quality and Testing Robotics, Romania, May **(2010),** pp. 1-5, 28-30.

[4] S. González-Vázquez and J. Moreno-Valenzuela, “A New Nonlinear PI/PID Controller for Quadrotor Posture Regulation”, September 28-October 1 **(2010)**, pp. 642-647, Mexico.

[5] M. Bouchoucha, S. Seghour and H. Osmani, “Integral Backstepping for Attitude Tracking of a Quadrotor System”, Electronics and Electrical Engineering, vol. 116, **(2011)**, pp. 75-80.

[6] A. Das, F. Lewis and K. Subbaro, “Backstepping approach for controlling a quadrotor using lagrange form dynamics”, Journal of Intelligent Robotic and System, vol. 56, **(2009)**, pp. 127-151.

[7] A.A. Mian and W. Daobo, “Modeling and Backstepping-based Nonlinear Control Strategy for a 6 DOF Quadrotor Helicopter”, Chinese Journal of Aeronautics, vol. 21, **(2008)**, pp. 261-268.

[8] T. Madani and A. Benallegue, “Backstepping Sliding Mode Control Applied to a Miniature Quadrotor Flying Robot”, 32nd Annual Conference on IEEE Industrial Electronics, November **(2006).**

[9] M. Bouchoucha, S. Seghour and H. Osmani, “Integral Backstepping for Attitude Tracking of a Quadrotor System”, Electronic and Electrical Engineering, vol. 10, no. 116, **(2010).**

[10] J. Escareño, S. Salazar, H. Romero and R. Lozano, “Trajectory Control of a Quadrotor Subject to 2D Wind Disturbances”, Journal of Intelligent Robotic System, vol. 70, **(2013)**, pp. 51-63.

[11] H. Liu, Y. Bai, G. Lu, Z. Shi and Y. Zhong, "Robust Tracking Control of a Quadrotor Helicopter", Journal of Intelligent & Robotic Systems, **(2013),** pp. 1-14.
[12] Raffo, V. Guilherme, M.G. Ortega and F.R. Rubio, "An integral predictive/ nonlinear H∞ control structure for a quadrotor helicopter", Automatica, vol. 46, no. 1, **(2010)**, pp. 29-39.
[13] M. Kerma, A. Mokhtari, B. Abdelaziz and Y. Orlov, "Nonlinear H∞ control of a Quadrotor (UAV), using high order sliding mode disturbance estimator", International Journal of Control, vol. 85, no. 12, **(2012)**, pp. 1876-1885.
[14] F. Zheng and W. Gao, "Adaptive integral backstepping control of a micro-quadrotor", Intelligent Control and Information Processing (ICICIP), 2nd International Conference on, IEEE, vol. 2, **(2011).**
[15] B.C. Min, J.H. Hong and E.T. Matson, "Adaptive Robust Control (ARC) for an Altitude Control of a Quadrotor Type UAV Carrying an Unknown Payloads", 11th International Conference on Control, Automation and Systems, Oct. 26-29, **(2011)**, Korea.
[16] C. Coza, C. Nicol, C.J.B. Macnab and A. Ramirez-Serrano, "Adaptive fuzzy control for a quadrotor helicopter robust to wind buffeting", Journal of Intelligent & Fuzzy Systems, vol. 22, **(2011)**, pp. 267-283.
[17] I. Fayçal, V.M. Fernández and J. Rodellar, "Adaptive Backstepping Control of a Class of Uncertain Nonlinear Systems: Application to Bouc-Wen Hysteretic Oscillators", CRM, **(2003)**
[18] C. Wang, M. Nahon and M. Trentini, "Controller development and validation for a small quadrotor with compensation for model variation", Unmanned Aircraft Systems (ICUAS), International Conference on IEEE, **(2014).**

Authors

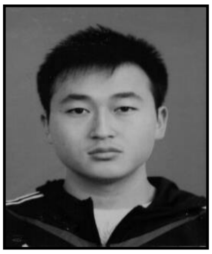

Chen Wang, He received the Bachelor and Master degree of Aircraft design in Aeronautical School form Northwestern Polytechnical University, Xi'an, China, in 2009. He is currently working towards the Ph.D degree at Northwestern Polytechnical University.

He worked as research trainee in Mechanical Engineering at McGill University, QC, Canada from 2012 to 2014. His current research interests include the area of dynamics and control of MAV system, with a focus on aerospace applications.

Song Bifeng, He received the B.A.Sc. and Ph.D. form Northwestern Polytechnical University, Xi'an, China.

He is a professor of Aeronautics of Northwestern Polytechnical University. His research directions include: conceptual design of aircraft, aircraft structure design, Near Space vehicle technology, Micro Air vehicle technology.

Meyer Nahon, He obtained a B.A.Sc. in Mechanical Engineering from Queen's University in Kingston, an M.A.Sc. in Aerospace Engineering from the University of Toronto, and a Ph.D. in Mechanical Engineering from McGill University in Montreal.

He was a faculty member in the Department of Mechanical Engineering at the University of Victoria from 1991 to 2001. Since then has been at McGill University, presently as a Professor of Mechanical Engineering. His research deals with various aspects of dynamics and control of aerial and marine vehicles and systems, with a particular emphasis on tethered systems.

He is a Senior Member of the IEEE, and an Associate Fellow of the AIAA and Fellow of the Canadian Aeronautics and Space Institute (CASI). He has received awards from the AIAA and CASI for his work on flight simulator motion systems and on space-based robotics.